



1 Lithium isotopes in dolostone as a palaeo-environmental
2 proxy – An experimental approach
3

4 Holly L. Taylor^{1,*}, Isaac J. Kell Duivesteyn², Juraj Farkaš^{3,4}, Martin Dietzel², Anthony Dosseto¹
5

6 ¹ Wollongong Isotope Geochronology Laboratory, School of Earth & Environmental Sciences.
7 University of Wollongong. Wollongong, NSW, Australia

8 ² Institute of Applied Geosciences. Graz University of Technology. Graz, Austria

9 ³ Department of Earth Sciences. University of Adelaide. Adelaide, SA, Australia

10 ⁴ Department of Environmental Geosciences, Faculty of Environmental Sciences, Czech
11 University of Life Sciences Prague, Kamycka 129, Praha – Suchbát, Czech Republic

12

13

14

15

16

17

18

19

20

21

22

23

24

25 * corresponding author: hlt434@uowmail.edu.au

26 **Abstract**

27 Lithium (Li) isotopes in marine carbonates have considerable potential as a proxy to constrain
28 past changes in silicate weathering fluxes and improve our understanding of Earth's climate.
29 To date the majority of Li isotope studies on marine carbonates have focussed on calcium
30 carbonates. Determination of the Li isotope fractionation between dolomite and a dolomitizing
31 fluid, would allow us to extend investigations to deep times (i.e., Precambrian) when
32 dolostones were the most abundant marine carbonate archives. Dolostones often contain a
33 significant proportion of detrital silicate material, which dominates the Li budget, thus pre-
34 treatment needs to be designed so that only the isotope composition of the carbonate-associated
35 Li is measured. This study aims to serve two main goals: (1) determining the Li isotope
36 fractionation between Ca-Mg carbonates and solution and (2) to develop a method for leaching
37 the carbonate-associated Li out of dolostone while not affecting that contained within the
38 detrital portion of the rock.

39 We synthesized Ca-Mg carbonates at high temperature (150 to 220 °C) and measured the Li
40 isotope composition ($\delta^7\text{Li}$) of precipitated solids and their respective reactive solutions. The
41 relationship of the Li isotope fractionation factor with temperature was obtained:

$$42 \quad 10^3 \ln \alpha_{\text{prec-sol}} = - \frac{(2.56 \pm 0.27) \times 10^6}{T^2} + (5.8 \pm 1.3)$$

43 Competitive nucleation and growth between dolomite and magnesite were observed during the
44 experiments, however, without notable effect of their relative proportion on the apparent Li
45 isotope fractionation. We found that Li isotope fractionation between precipitated solid and
46 solution is much greater for Ca-Mg carbonates than for Ca carbonates. If the seawater
47 temperature can be estimated independently, the above equation could be used in conjunction
48 with the Li isotope composition of dolostones to derive those of the precipitating solutions and
49 hence make inferences about the past oceanic Li cycle.



50 In addition, we also conducted leaching experiments on a Neoproterozoic dolostone and a
51 Holocene coral. Results show that leaching with 0.05M HCl or 0.5% acetic acid at room
52 temperature for 60 min releases Li from the carbonate fraction without significant contribution
53 of Li from the siliciclastic detrital component.

54 These experimental and analytical developments provide a basis for the use of Li isotopes in
55 dolostones as a palaeo-environmental proxy, which will contribute to further advance our
56 understanding of the evolution of Earth's surface environments.

57

58 **1. Introduction**

59 Lithium isotopes in marine carbonates have emerged as a powerful proxy to understand the
60 evolution of the ocean chemistry, past silicate weathering fluxes and their links to global
61 climate. Application to calcium carbonates (e.g. foraminifera, limestone) has shed some light
62 on hotly debated topics such as, the evolution of Earth's climate during the Cenozoic (Misra
63 and Froelich, 2012; Li and West, 2014; Wanner et al., 2014; Vigier and Godd  ris, 2015; Hathorne
64 and James, 2006), oceanic anoxic events (Pogge von Strandmann et al., 2013b; Lechler et al.,
65 2015) and Palaeozoic glaciation (Pogge von Strandmann et al., 2017). Although post-
66 depositional alteration can play an important role in the formation of dolomite (Geske et al.,
67 2012; Burns et al., 2000), the application of Li isotopes to marine dolostone could help to extend
68 our understanding of the geochemical evolution of ancient seawater, particularly in early Earth
69 geological history (i.e., Precambrian).

70

71 While data of Li isotopic fractionation during calcite precipitation has been relatively well
72 constrained (Marriott et al., 2004a; Marriott et al., 2004b; Dellinger et al., 2018), there is
73 currently no data available pertaining to Li isotope fractionation during dolomite formation.
74 Therefore in this study, precipitation experiments were carried out at various temperatures



75 (150–220 °C), where the Li isotopic composition of the precipitated solids and their respective
 76 reactive solutions were subsequently measured in order to determine the fractionation factor
 77 between the fluid and solid phases. The experiments were conducted at elevated temperatures
 78 due to the impossibility of synthesizing well-ordered dolomite at ambient temperatures on a
 79 laboratory time scale (Land, 1998; Arvidson and Mackenzie, 1999; Gregg et al., 2015).

80

81 One major difficulty with interpreting Li isotopes in dolostone is that they often contain a
 82 significant proportion of siliciclastic material (e.g. detrital micas and/or authigenic clay
 83 minerals). The abundance of Li in silicate minerals is higher than in carbonates (typically more
 84 than two orders of magnitudes), thus sample pre-treatment must be undertaken to extract Li
 85 from only the carbonate fraction (Pogge von Strandmann et al., 2013b). Therefore, in this study
 86 we have tested various pre-treatment methods in order to refine a procedure that faithfully
 87 yields the isotopic composition of the carbonate-associated Li fraction in dolostones
 88 exclusively.

89

90 **2. Methods**

91 *2.1. Ca-Mg carbonate synthesis*

92 Synthesis of Ca-Mg carbonates was conducted in Teflon-lined, stainless steel
 93 autoclaves at temperatures of 150, 180 and 220°C ($\pm 5^\circ\text{C}$) through the reaction of ~300 mg of
 94 powdered inorganic aragonite (speleothem aragonite; in-house mineral collection at Graz
 95 University of Technology) with an artificial brine solution containing 200 mM Mg, 0.245 mM
 96 Li and 50 mM NaHCO_3 . The reactive fluid was prepared by dissolving analytical grade
 97 $\text{MgCl}_2 \cdot 6\text{H}_2\text{O}$ (Roth; $\geq 99\%$, p.a., ACS), LiCl (Merck; $\geq 99\%$, ACS, Reag. Ph Eur) and NaHCO_3
 98 (Roth; $\geq 99.5\%$, p.a., ACS, ISO) in ultrapure water (Millipore Integral 3: $18.2\text{ M}\Omega\text{cm}^{-1}$). The
 99 stock solution was subsequently filtered through a $0.45\text{ }\mu\text{m}$ cellulose acetate membrane filter



(Sartorius). The reagent inorganic aragonite was milled to a grain size $< 20 \mu\text{m}$ using a vibratory mill (McCrone Micronizing Mill) for 10 minutes and collected by dry sieving prior to use in the experiments. Autoclaves were sealed immediately after mixing the inorganic aragonite with the appropriate volume of stock solution and placed in preheated ovens.

Samples were taken from the autoclaves at each operating temperature after a given reaction time (Table 1), including repeat samples. Upon removal from heat, the reactors were quenched and the samples were subsequently filtered through a $0.2 \mu\text{m}$ cellulose acetate membrane (Sartorius) using a vacuum filtration unit. Samples were then thoroughly rinsed with ultrapure water (Millipore Integral 3: $18.2 \text{ M}\Omega\cdot\text{cm}^{-1}$) to remove any soluble salts from the matrix and subsequently dried in an oven at 40°C overnight to be ready for solid phase analysis. An aliquot of the reactive fluid was acidified to a $\sim 3\%$ HNO_3 matrix for elemental and Li isotope analyses using Merck® Suprapur™ HNO_3 .

2.2. Leaching experiments

A Neoproterozoic dolostone from the Nuccaleena Formation (Flinders Ranges, South Australia) and a Holocene *Porites* coral were used to evaluate the effect of different leaching protocols on the measured Li isotope composition. Samples were ground to a powder using a TEMA chromium-ring grinding mill. An aliquot of powdered dolostone was used for mineralogy quantification performed using X-ray diffraction. Another aliquot of one gram was placed in a clean polypropylene centrifuge tube and 20 mL of solution was added. Leaching was tested with hydrochloric acid (HCl) of varying concentrations (0.05M, 0.1M, 0.15M, 0.2M, 0.3M, 0.5, 0.8M, 1M, 6M) and acetic acid (HAc) at concentrations of 0.5 and 2 %. Acetic acid and HCl solutions were prepared from trace grade glacial acetic acid (Merck® Suprapur™) and ultra-trace grade 30% HCl (Merck® Ultrapur™). In each case, the powder and solution reacted at room temperature for one hour, while continuous mixing was achieved



125 with an orbital shaker. The supernatant fluid was separated by centrifugation at 4000 rpm for
126 15 minutes. After separation, the supernatant fluid was extracted using acid-washed disposable
127 pipettes. An aliquot containing ~60 ng of Li was subsequently sampled for cation exchange
128 chromatography.

129 2.3. *Mineralogy quantification*

130 Quantitative phase contents of the synthesized solids were determined by powder X-
131 ray diffraction (XRD) of finely ground aliquots performed on a PANalytical X'Pert PRO
132 diffractometer outfitted with a Co-target tube (operated at 40 kV and 40 mA), a high-speed
133 Scientific X'Celerator detector, 0.5° antiscattering and divergence slits, spinner stage, primary
134 and secondary soller and automatic sample changer. Samples were finely ground by hand using
135 a mortar and pestle prior to analysis and were loaded in a random orientation using the top
136 loading technique. The samples were analysed over the range 4 – 85° 2θ with a step size of
137 0.008° 2θ and a count time of 40 seconds/step. Mineral quantification was obtained by Rietveld
138 Refinement of the XRD patterns using the PANalytical X'Pert HighScore Plus Software and
139 its implemented pdf-2 database.

140

141 2.4. *Elemental concentrations*

142 Lithium concentrations of solutions were analysed in acidified (0.3 M HNO₃) aliquots
143 by inductively coupled plasma optical emission spectroscopy (ICP-OES) using a PerkinElmer
144 Optima 8300. A range of in-house and NIST 1640a standards were measured at the beginning
145 and end of a sample series, with an estimated analytical error (2σ, 3 replicates) of ±3% relative
146 to the standard. For synthesized solids, an aliquot of each precipitate was dissolved in 0.9 M
147 HNO₃ at 70°C for 12 hours in an ultrasonic bath to ensure complete digestion. Subsequently Li
148 concentrations were analysed by ICP-OES following the same method as for the aqueous
149 solutions.

150

151 2.5. *Lithium isotopes*

152 Sample preparation for Li isotope measurement was undertaken in a Class 100
153 cleanroom at the Wollongong Isotope Geochronology Laboratory, University of Wollongong.
154 For mineral precipitates, the samples were ground using a mortar and pestle before aliquots of
155 <0.05 g were weighed. The sample aliquots were dissolved in dilute HNO₃ (Ultrapur™) and
156 0.2 mL of concentrated H₂O₂ (31% Ultrapur™) was added to ensure the breakdown of organics.
157 The samples were then placed on a hotplate overnight at 50°C to reflux and ensure complete
158 digestion of the solids. After complete digestion of the solids, Li concentrations were measured
159 by Quadrupole ICP-MS. An aliquot of the digested samples containing ~60 ng of Li was then
160 dried down and taken up into 1.5 mL of Ultrapur™ 1 M HCl. Samples were then treated with
161 a two-step cation exchange chromatography procedure, following the methods of Balter and
162 Vigier (2014) to separate Li from the sample matrix. For Li isotope measurements it is crucial
163 that 100% of Li is recovered from the cation exchange columns as $\delta^7\text{Li}$ compositions have been
164 shown to vary by up to ~200 ‰ during chromatography due to incomplete recovery (Pistiner
165 and Henderson, 2003). It is also crucial to remove elements such as Na and Ca as large amounts
166 of Ca can coat the cones of the mass spectrometer while Na can reduce Li ionisation in the
167 plasma, and cause further Li isotopic fractionation during analysis (James and Palmer, 2000).
168 For chromatography, 30 mL Savillex micro columns (6.4 mm internal diameter, 9.6 cm outside
169 diameter, 25 cm capillary length) were used together with Biorad AG50W-X8 resin as the
170 cation exchange medium (volume = 3.06 cm³). The columns were calibrated with seawater
171 prior to treating the samples to verify that the procedure yielded 100% of the Li (Table A1).
172 The columns were cleaned with 30 mL of 6M HCl, rinsed with ~2 mL of MilliQ™ water and
173 conditioned using 8 mL of titrated, 1 M Ultrapur™ HCl before sample loading. To ensure the
174 complete removal of interfering elements from the Li, samples were passed through the
175 columns twice; after the first elution, the samples were dried down, taken up in 1 M HCl and



reloaded into the columns. The Li elutions were dried down and subsequently re-dissolved in Ultrapur™ 0.3M HNO₃ ready for isotopic analysis. Lithium isotope ratios were measured by multi collector inductively coupled plasma mass spectrometry (MC ICP-MS) on a ThermoFisher Neptune Plus at the Wollongong Isotope Geochronology Laboratory, University of Wollongong. A 30 ppb solution of IRMM-16 Li isotopic standard was used at the start of each measurement session to tune the instrument. An intensity of ~1 V was routinely obtained for ⁷Li, while the background ⁷Li intensity was between 5-30 mV. During analysis, standard bracketing, using IRMM-16 as the primary standard, was applied to correct the measured ⁷Li/⁶Li values for mass bias (Flesch et al., 1973). Instrumental blanks were measured before each sample so that background signal could be accounted for. The ⁷Li/⁶Li ratios were converted to δ⁷Li values using L-SVEC as reference to (Carignan et al., 2007) (Eq.(1)).

$$\delta^7\text{Li} = \left\{ \frac{\left(\frac{^7\text{Li}}{^6\text{Li}} \right)_{\text{sample}}}{\left(\frac{^7\text{Li}}{^6\text{Li}} \right)_{\text{L-SVEC}}} - 1 \right\} \cdot 1000 \quad (1)$$

The accuracy of analysis was assessed using synthetic solutions Li6-N and Li7-N (Carignan et al., 2007) as secondary standards every 6 samples. The accuracy of chromatography and analysis was assessed using a seawater standard (Table A1). External uncertainty on δ⁷Li compositions (at 2σ level) was evaluated by measurement of precipitated solids and solutions from repeat experiments at 150 °C (n = 3) and 180 °C (n = 2), amounting to 0.86 ‰ for precipitated solids and 1.2 ‰ for solutions.

3. Results

3.1. Precipitation experiments

Synthesized minerals are comprised of dolomite and magnesite (Table 1); their relative amount shows a relationship with temperature, with higher reaction temperatures yielding more magnesite and less dolomite compared to lower temperatures (Fig. 1). The Li concentration of



reactive solutions ranges from 1,666 to 3,695 $\mu\text{g}\cdot\text{L}^{-1}$ (Table A2) and shows no correlation with reaction temperature. On the contrary, the Li concentration of precipitated solids decreases with increasing temperature (from 25.9 to 8.20 ppm; Table A2).

The $\delta^7\text{Li}$ of the initial reactive solution is 7.85 ‰ (Table 2). After reaction the $\delta^7\text{Li}$ value of the solution ($\delta^7\text{Li}_{\text{sol}}$) vary between 7.87 and 9.48 ‰, while the $\delta^7\text{Li}$ values in the precipitated solid ($\delta^7\text{Li}_{\text{prec}}$) range from -0.63 to 3.08 ‰ (Table 2). The precipitated solids are 4.79 to 8.6 ± 0.6 ‰ (1σ ; $n=3$) lighter than the solution, and this difference (termed $10^3\cdot\ln\alpha_{\text{prec-sol}}$) increases with decreasing temperature (Table 2).

The Li isotope fractionation factor between the precipitated solid and the solution (calculated as $10^3\cdot\ln\alpha_{\text{prec-sol}} = 10^3\cdot\ln(1000+\delta^7\text{Li}_{\text{prec}}/1000+\delta^7\text{Li}_{\text{sol}})$) displays values within error of each other, despite a wide range of concentrations of dolomite or magnesite precipitated (Fig. 2). Similarly, there is no relationship between the Li distribution coefficient between precipitated solid and solution ($D_{[\text{Li}]\text{prec-sol}} = [\text{Li}]_{\text{prec}}/[\text{Li}]_{\text{sol}}$, where $[\text{Li}]_{\text{prec}}$ and $[\text{Li}]_{\text{sol}}$ are the Li concentrations in the precipitated solid and the solution, respectively), and mineral abundances (Fig. 3). Conversely, there is a positive relationship between $10^3\cdot\ln\alpha_{\text{prec-sol}}$ and the reaction temperature (Fig. 4).

3.2. Leaching experiments

For the dolostone, $\delta^7\text{Li}$ values of the leaching solution decrease from 9.5 to 4.0 ‰, with increasing HCl concentration (Table 3; Fig. 5a). The Al/Mg ratio in the leaching solutions increases at HCl concentrations >0.8 M from ~ 0.0009 to 0.01 (Fig. 5b). The leaching solutions show an increase in Li/Ca ratio from 6.3×10^{-6} to 25×10^{-6} with decreasing $\delta^7\text{Li}$ (Fig. 6a). Furthermore, the Li/Mg ratio increases from 5 to 12×10^{-5} with increasing $\delta^7\text{Li}$ (Fig. 6b). Very little carbonate minerals other than dolomite (1.1 wt % calcite and 2.1 wt % ankerite) are present in the dolostone sample, and the silicate minerals represents ~ 26 wt % of the sample



(14 wt % quartz, 6.2 wt % muscovite and 5.1 wt% albite) (Table A3). Leaching with acetic acid yields $\delta^7\text{Li}$ compositions in the solution similar to values observed in very dilute HCl (Fig. 7). The $\delta^7\text{Li}$ of the 2% HAc leaching solution is lower than that of the 0.5 % HAc leaching solution.

For the Holocene coral, the sample is dominated by aragonite (Table A4) and the leaching solution shows a similar trend to that from the dolostone leaching experiment, with $\delta^7\text{Li}$ values decreasing from 20.1 to 16.9 ‰ with increasing HCl concentration (Table 3; Fig. 8). Total dissolution of the coral yields a $\delta^7\text{Li}$ value in the solution of 20.6‰, which is within error of the values determined for HCl leaching experiments with acid concentrations <0.5 M (Table 3).

235

236 4. Discussion

237 4.1. Lithium isotope fractionation during inorganic precipitation of Ca-Mg carbonate

The precipitated solids of the synthesis experiments consist of Mg-Ca carbonates with variable amounts of dolomite ($\text{CaMg}(\text{CO}_3)_2$) and magnesite (MgCO_3) (Table 1). The $\delta^7\text{Li}$ composition of the precipitated solid is systematically isotopically lighter than that of the reactive solution (Table 2). These results are consistent with previous experimental work on Li isotope fractionation during calcite precipitation (Marriott et al., 2004a; Marriott et al., 2004b), which showed that the Li isotope composition of calcite is isotopically lighter than that of the corresponding fluid. Teng et al. (2008) have suggested that the incorporation of ^6Li over ^7Li in minerals compared to the growth solution reflects a change from four- to six-fold coordination of Li during mineral growth. In calcite from foraminifera and aragonite from corals, $\delta^7\text{Li}$ values are respectively about 3 and 11 ‰ lower compared to their growth solutions (Marriott et al., 2004a). Here, the precipitated minerals are 4.8 to 8.6 ± 0.6 ‰ (1σ ; $n=3$) lighter than the solution. This difference increases with decreasing temperature, as would be expected for



250 stable isotope fractionation at equilibrium. As our experiments were conducted at high
251 temperatures, the system can be reasonable considered to be approaching isotope equilibrium
252 conditions as fractionation scales with the inverse of reaction temperature (see Fig. 3). Marriott
253 et al. (2004a) suggested that Li isotope fractionation probably occurs at equilibrium even at
254 lower temperatures for several reasons: (i) kinetic fractionation would probably be much
255 greater (up to ~80 ‰) than that observed (both in calcite and in Ca-Mg carbonate), thus
256 requiring boundary layer processes or the presence of a back-reaction, for which there is no
257 evidence. (ii) Observed isotopic fractionation between calcite and growth solution, as well as
258 between Ca-Mg carbonate and growth solution, are consistent with ab initio calculations for
259 equilibrium fractionation (Yamaji et al., 2001). (iii) Lithium isotope fractionation between
260 calcite and growth solution is relatively constant across a wide range of concentration of Li
261 incorporated in calcite (this was not tested here).

262 Although Li isotope fractionation and the magnesite:dolomite ratio of the precipitated
263 solid both co-vary with temperature, there is no relationship between the $\delta^7\text{Li}$ composition of
264 the precipitate solids or that of their respective reactive solutions and the magnesite:dolomite
265 ratio of the precipitate solid (not shown). This suggests that the nature of the Ca-Mg carbonate
266 precipitated does not have a significant influence on Li isotope fractionation. This hypothesis
267 is supported by the absence of significant variation in the Li isotope fractionation factor
268 ($10^3\ln\alpha_{\text{prec-sol}}$; Fig. 2) or the Li distribution coefficient between solid and solution ($D_{[\text{Li}]_{\text{prec-sol}}}$;
269 Fig. 3), despite a wide range of mineral abundances. For instance, most $10^3\ln\alpha_{\text{prec-sol}}$ values are
270 within error of each other while dolomite concentration varies from 17 to 82 wt % (Fig. 2a).
271 This differs from what Marriott et al. (2004b) observed for calcium carbonates at ambient
272 temperature, where the isotopic fractionation is aragonite (~11 ‰) was much greater than in
273 calcite (~3 ‰).



274 The relationship between $10^3 \ln \alpha_{\text{prec-sol}}$ and temperature can be used to estimate the
 275 temperature dependency for Li isotope fractionation between Ca-Mg carbonate and solution.
 276 Using average $10^3 \ln \alpha_{\text{prec-sol}}$ values for each reaction temperature, we obtain the following
 277 temperature-dependent relationship:

$$278 \quad 10^3 \ln \alpha_{\text{prec-sol}} = -\frac{(2.56 \pm 0.27) \times 10^6}{T^2} + (5.8 \pm 1.3) \quad (2)$$

279 where T is the temperature of precipitation in K.

280 Using Eq. (2), the Li isotopic fractionation at 25 °C is estimated to be $-23.0 \pm 5.7 \text{ ‰}$
 281 (1σ) (Fig. 4). Although there is a large error on this estimate, our results suggest that Li
 282 isotopic fractionation during dolomite/magnesite precipitation is significant larger than
 283 during calcium carbonate precipitation (Marriott et al., 2004a).

284 If the temperature of the solution from which dolomite is precipitated can be known or
 285 calculated (e.g., via clumped Δ_{47} proxy, Winkelstern et al. 2016), the above relationship in
 286 combination with the $\delta^7\text{Li}$ of marine dolostone could be used to determine the Li isotopic
 287 composition of the precipitating palaeo-solution, e.g. brine or seawater. It is important to note
 288 that the applicability to natural systems may be limited to dolomite precipitated inorganically,
 289 as it has been proposed that bacterial mediation could play a major role in the precipitation of
 290 dolomite from natural waters at ambient conditions (Vasconcelos et al., 1995). In addition,
 291 marine dolomite is often of secondary origin, as a result of diagenetic replacement of calcium
 292 carbonate, thus a syn-depositional origin for dolomite must be ascertained before its $\delta^7\text{Li}$
 293 composition can be used to estimate that of seawater.

294

295 4.2. Extraction of carbonate-bound Li in dolostones

296 Leaching of dolostone with solutions of variable HCl concentrations yields $\delta^7\text{Li}$
 297 compositions of the leaching solution that decrease with increasing HCl concentrations,
 298 suggesting an increasing contribution of isotopically light Li from detrital silicates, such as clay



minerals (Fig. 5a). This hypothesis is supported by a negative relationship between $\delta^7\text{Li}$ values and Li/Ca ratios of the leaching solutions (Fig. 6), similarly to results from leaching experiments on the Plenus Marl Limestone (Pogge von Strandmann et al., 2013a). The Li/Ca ratio is used instead of Li/Mg because Mg is also present in silicate minerals. Indeed, $\delta^7\text{Li}$ and Li/Mg ratios show a positive relationship (Fig. 8b), surprisingly suggesting that dolomite and the detrital component are characterised by high and low Li/Mg ratios, respectively.

The increasing contribution of silicate minerals with the increasing HCl concentration of the leaching solution is further illustrated by increasing Al/Mg ratios in the leaching solution (Fig. 5b). The contribution from silicates becomes significant for HCl concentrations >0.5 M. For HCl concentrations <0.8 M, the relationship between Al/Mg and HCl concentration breaks down (Fig. 5b), indicating that silicates have a negligible role on the composition of the solution. Nevertheless, $\delta^7\text{Li}$ values decrease for HCl concentrations as low as 0.1 M. Thus, we propose that treatment of dolostone with a solution of 0.05 M HCl at room temperature for 60 mins, is the best compromise between minimising the contribution of silicates and obtaining enough Li for isotopic analysis.

Leaching experiments were also conducted on a *Porites* coral of Holocene age to test the proposed protocol, since the $\delta^7\text{Li}$ of modern coral is known (Marriott et al., 2004a; Rollion-Bard et al., 2009). Furthermore, because the aragonitic skeleton of modern corals is generally free of detrital material, we can also test that the chosen leaching protocol yields the same Li isotopic composition in the resulting solution, as with total dissolution of the coral. Total dissolution of the modern coral yields a $\delta^7\text{Li}$ value of 20.6 ‰ (Fig. 8). Leaching solutions with HCl concentrations <0.5 M HCl exhibit $\delta^7\text{Li}$ values within error of that obtained from total dissolution. These values are also consistent with $\delta^7\text{Li}$ compositions between 18.4 and 19.6 ‰ measured in *Porites*, and 21 ‰ in *Acropora* corals (Marriott et al., 2004a). Biomineralization has no major effect on the incorporation of Li in coral or foraminifera as Li has no known



biological function. The Li isotopic difference between coral and seawater is ~ 11 ‰ (Marriott et al., 2004a). Therefore, $\delta^7\text{Li}$ values obtained from the total dissolution and for leaching solutions with a HCl concentration < 0.5 M would yield a $\delta^7\text{Li}$ composition for modern seawater of 31‰, consistent with published values (Misra and Froelich, 2012). Consequently, these results suggest that leaching with a 0.05 M HCl solution is appropriate to derive the Li associated to the carbonate fraction only.

Interestingly both coral and dolostone leaching solutions show a decrease in $\delta^7\text{Li}$ values with increasing HCl concentration. This is surprising since the coral is at 97 % aragonite (2 % magnesite and 1% calcite) so the release of isotopically light Li from silicates is not expected. These results imply that total dissolution in dilute HNO_3 does not release isotopically light Li into solution, which could be contained in organic colloids, since no residue was observed. The lack of relationship between $\delta^7\text{Li}$ values and Li/Ca ratios (Fig. A1) suggests that this isotopically light Li is not bound to silicates (which would have a very different Li/Ca from aragonite). In the coral, this pool of Li remains unidentified. However, as shown above, leaching with solutions with < 0.5 M HCl yield Li isotope compositions expected for a coral in equilibrium with the modern seawater.

Leaching of dolostone with acetic acid yields $\delta^7\text{Li}$ compositions in the solution similar to that of solutions with a HCl concentration ≤ 0.1 M (Fig. 7). The $\delta^7\text{Li}$ composition of the 2% HAc solution is lower (8.37 ‰) than that of the 0.5% HAc solution, which could maybe suggest a contribution from silicate-bound Li. Thus, treatment of dolostone with a solution of 0.5% HAc at room temperature for 60 mins could be an alternative method to derive carbonate-bound Li.

346
347
348



349 5. Summary and Conclusions

350 Precipitation experiments at high temperature yielded dolomite and magnesite in
351 variable proportions. However, varying mineralogy does not seem to measurably impact Li
352 isotopic fractionation between the carbonate and the solution. The Li isotopic composition of
353 the precipitated solid is isotopically lighter than the reactive solution, similarly to previous
354 experiments on calcium carbonates (Marriott et al., 2004b; Marriott et al., 2004a). The isotope
355 fractionation factor is mainly controlled by temperature, which in turn allows us to calculate
356 the Li isotopic composition of the solution using $\delta^7\text{Li}$ value of the Ca-Mg carbonate, if the
357 precipitation temperature can be estimated independently (e.g. oxygen or clumped isotope
358 thermometry). Thus, the temperature dependant relationship in Eq. (2) could be useful for
359 reconstructing $\delta^7\text{Li}$ of palaeo-seawater and/or dolomitizing fluids (i.e., reactive solution) as an
360 approximation based on the Li isotope composition of dolostones in geological records.

361 Leaching experiments show that it is possible to selectively dissolve the carbonate-bound
362 Li in dolostones by using 0.05 M HCl or 0.5% acetic acid at room temperature for 60 min.
363 Leaching of coral with 0.05M HCl shows that this protocol yields a Li isotope composition for
364 the solution representative of that of the carbonate minerals. Thus, the described protocol
365 allows us to derive the Li isotope composition of the carbonate fraction of dolostones while
366 leaving the Li from any co-present silicates intact.

367 Combined results from leaching and precipitation experiments show that future studies of
368 Li isotopes in dolostones have high potential to further constraints the evolution of the Li
369 isotopic composition of ancient precipitation fluids, like ocean and brines, thus improve our
370 understanding of changes in the Earth's palaeo-environments.

371

372



373 Appendix A

374 Table A1. Column calibration using seawater samples

Column ID	$\delta^7\text{Li}$ (‰)
Column A	31.1 ± 0.08
Column C	20.9 ± 0.08
Column D	31.6 ± 0.1
Column E	29.9 ± 0.08
Column F	31.7 ± 0.1
Column G	29.5 ± 0.07
Column H	30.7 ± 0.1
Column I	30.9 ± 0.1
Column J	30.9 ± 0.09
Column K	30.8 ± 0.09
Column L	32.0 ± 0.1
Column M	31.3 ± 0.1
Column N	30.7 ± 0.1
Column O	30.1 ± 0.1
Column P	30.8 ± 0.06
Column Q	30.6 ± 0.07
Column R	28.8 ± 0.08
Column S	31.1 ± 0.09
Column Z	29.3 ± 0.08

375
 376 Errors are internal analytical uncertainties reported at the 2σ level. Column C was not used due to the $\delta^7\text{Li}$ value
 377 being significantly different from the seawater value.
 378

379 Table A2. Concentrations of lithium in reactive fluids and precipitated solids

Sample ID	$[\text{Li}]_{\text{sol}}$ ($\mu\text{g. L}^{-1}$)	$[\text{Li}]_{\text{prec}}$ (ppm)
LiDol – 150 – 4.1	3,695	25.9
LiDol – 150 – 4.2	3,415	20.5
LiDol – 150 – 4.3	3,036	21.8
LiDol – 180 – 4.1	3,434	16.0
LiDol – 180 – 4.2	3,238	15.7
LiDol – 220 – 3	1,666	8.20

380
 381
 382
 383
 384
 385
 386
 387
 388



389 Table A3. Mineral concentration of Nuccaleena dolostone (EC26) used in the leaching
390 experiment

391

Mineral	Concentration (wt %)
Quartz	14
Albite	5.1
Calcite	1.1
Dolomite	70
Ankerite	2.1
Siderite	0.2
Kaolinite	1.0
Chlorite	0.2
Muscovite	6.2

392

393

394 Table A4. Mineral concentrations of coral used in the leaching experiment

395

Mineral	Concentration (wt %)
Aragonite	97
Calcite	1.0
Dolomite	0.4
Magnesite	1.6

396

397



398 **Author contribution**

399 HLT, AD, JF and MD designed the project; MD and IJKD conducted the precipitation
400 experiments; HLT conducted the leaching experiments and all other analytical work; HLT and
401 AD wrote the manuscript; all authors edited the manuscript.

402

403 **Acknowledgements**

404 We would like to thank Jasmine Hunter and Helen McGregor (University of Wollongong) for
405 providing the coral samples, Alexander Corrick (University of Adelaide) for help collecting
406 the Nuccaleena dolomite samples and Andre Baldermann (Graz University of Technology) for
407 performing the Li concentration analytics. The laboratory precipitation experiments and
408 fieldwork related to this study was supported by the *Base-Line Earth* project (ITN MC Horizon
409 2020, grant agreement No. 643084), Czech Science Foundation (GACR grant No. 17-18120S),
410 Australian Government Research Training Program and ARC Linkage Project LP160101353.



411 References

- 412 Arvidson, R. S., and Mackenzie, F. T.: The dolomite problem; control of precipitation kinetics
413 by temperature and saturation state, *American Journal of Science*, 299, 257-288, 1999.
- 414 Balter, V., and Vigier, N.: Natural variations of lithium isotopes in a mammalian model,
415 *Metallomics*, 6, 582-586, 2014.
- 416 Burns, S. J., McKenzie, J. A., and Vasconcelos, C.: Dolomite formation and biogeochemical
417 cycles in the Phanerozoic, *Sedimentology*, 47, 49-61, 2000.
- 418 Carignan, J., Vigier, N., and Millot, R.: Three Secondary Reference Materials for Lithium
419 Isotope Measurements: Li7-N, Li6-N and LiCl-N Solutions, *Geostandards and Geoanalytical
420 Research*, 31, 7-12, 2007.
- 421 Dellinger, M., West, A. J., Paris, G., Adkins, J. F., von Strandmann, P. A. P., Ullmann, C. V.,
422 Eagle, R. A., Freitas, P., Bagard, M.-L., and Ries, J. B.: The Li isotope composition of marine
423 biogenic carbonates: Patterns and Mechanisms, *Geochimica et Cosmochimica Acta*, 2018.
- 424 Flesch, G., Anderson, A., and Svec, H.: A secondary isotopic standard for 6Li/7Li
425 determinations, *International Journal of Mass Spectrometry and Ion Physics*, 12, 265-272,
426 1973.
- 427 Geske, A., Zorlu, J., Richter, D., Buhl, D., Niedermayr, A., and Immenhauser, A.: Impact of
428 diagenesis and low grade metamorphism on isotope (δ 26 Mg, δ 13 C, δ 18 O and 87 Sr/86 Sr)
429 and elemental (Ca, Mg, Mn, Fe and Sr) signatures of Triassic sabkha dolomites, *Chemical
430 Geology*, 332, 45-64, 2012.
- 431 Gregg, J. M., Bish, D. L., Kaczmarek, S. E., and Machel, H. G.: Mineralogy, nucleation and
432 growth of dolomite in the laboratory and sedimentary environment: a review, *Sedimentology*,
433 62, 1749-1769, 2015.
- 434 Hathorne, E. C., and James, R. H.: Temporal record of lithium in seawater: A tracer for silicate
435 weathering?, *Earth and Planetary Science Letters*, 246, 393-406, 2006.
- 436 James, R. H., and Palmer, M. R.: The lithium isotope composition of international rock
437 standards, *Chemical Geology*, 166, 319-326, 2000.
- 438 Land, L. S.: Failure to Precipitate Dolomite at 25 C from Dilute Solution Despite 1000-Fold
439 Oversaturation after 32 Years, *Aquatic Geochemistry*, 4, 361-368, 1998.
- 440 Lechler, M., Pogge von Strandmann, P. A. E., Jenkyns, H. C., Prosser, G., and Parente, M.:
441 Lithium-isotope evidence for enhanced silicate weathering during OAE 1a (Early Aptian Selli
442 event), *Earth and Planetary Science Letters*, 432, 210-222,
443 <http://dx.doi.org/10.1016/j.epsl.2015.09.052>, 2015.
- 444 Li, G., and West, A. J.: Evolution of Cenozoic seawater lithium isotopes: Coupling of global
445 denudation regime and shifting seawater sinks, *Earth and Planetary Science Letters*, 401, 284-
446 293, <http://dx.doi.org/10.1016/j.epsl.2014.06.011>, 2014.
- 447 Marriott, C. S., Henderson, G. M., Belshaw, N. S., and Tudhope, A. W.: Temperature
448 dependence of δ 7 Li, δ 44 Ca and Li/Ca during growth of calcium carbonate, *Earth and
449 Planetary Science Letters*, 222, 615-624, 2004a.
- 450 Marriott, C. S., Henderson, G. M., Crompton, R., Staubwasser, M., and Shaw, S.: Effect of
451 mineralogy, salinity, and temperature on Li/Ca and Li isotope composition of calcium
452 carbonate, *Chemical Geology*, 212, 5-15, 2004b.
- 453 Misra, S., and Froelich, P. N.: Lithium isotope history of Cenozoic seawater: Changes in
454 silicate weathering and reverse weathering, *Science*, 335, 818-823, DOI
455 10.1126/science.1214697, 2012.
- 456 Pistiner, J. S., and Henderson, G. M.: Lithium-isotope fractionation during continental
457 weathering processes, *Earth and Planetary Science Letters*, 214, 327-339, 2003.



- 458 Pogge von Strandmann, P. A., Jenkyns, H. C., and Woodfine, R. G.: Lithium isotope evidence
459 for enhanced weathering during Oceanic Anoxic Event 2, *Nature Geoscience*, 6, 668-672,
460 2013a.
- 461 Pogge von Strandmann, P. A. E., Jenkyns, H. C., and Woodfine, R. G.: Lithium isotope
462 evidence for enhanced weathering during Oceanic Anoxic Event 2, *Nature Geosci*, 6, 668-672,
463 10.1038/ngeo1875
464 <http://www.nature.com/ngeo/journal/v6/n8/abs/ngeo1875.html#supplementary-information>,
465 2013b.
- 466 Pogge von Strandmann, P. A. E., Desrochers, A., Murphy, M. J., Finlay, A. J., Selby, D., and
467 Lenton, T. M.: Global climate stabilisation by chemical weathering during the Hirnantian
468 glaciation, *Geochemical Perspectives Letters*, 230-237, 10.7185/geochemlet.1726, 2017.
- 469 Rollion-Bard, C., Vigier, N., Meibom, A., Blamart, D., Reynaud, S., Rodolfo-Metalpa, R.,
470 Martin, S., and Gattuso, J.-P.: Effect of environmental conditions and skeletal ultrastructure on
471 the Li isotopic composition of scleractinian corals, *Earth and Planetary Science Letters*, 286,
472 63-70, 2009.
- 473 Teng, F.-Z., Rudnick, R. L., McDonough, W. F., Gao, S., Tomascak, P. B., and Liu, Y.:
474 Lithium isotopic composition and concentration of the deep continental crust, *Chemical*
475 *Geology*, 255, 47-59, <http://dx.doi.org/10.1016/j.chemgeo.2008.06.009>, 2008.
- 476 Vasconcelos, C., McKenzie, J. A., Bernasconi, S., Grujic, D., and Tiens, A. J.: Microbial
477 mediation as a possible mechanism for natural dolomite formation at low temperatures, *Nature*,
478 377, 220, 10.1038/377220a0, 1995.
- 479 Vigier, N., and Godd  ris, Y.: A new approach for modeling Cenozoic oceanic lithium isotope
480 paleo-variations: the key role of climate, *Climate of the Past*, 11, 635-645, 10.5194/cp-11-635-
481 2015, 2015.
- 482 Wanner, C., Sonnenthal, E. L., and Liu, X.-M.: Seawater $\delta^7\text{Li}$: A direct proxy for global CO₂
483 consumption by continental silicate weathering?, *Chemical Geology*,
484 <http://dx.doi.org/10.1016/j.chemgeo.2014.05.005>, 2014.
- 485 Yamaji, K., Makita, Y., Watanabe, H., Sonoda, A., Kanoh, H., Hirotsu, T., and Ooi, K.:
486 Theoretical estimation of lithium isotopic reduced partition function ratio for lithium ions in
487 aqueous solution, *The Journal of Physical Chemistry A*, 105, 602-613, 2001.
- 488



Figure captions

Figure 1. a) Dolomite and b) magnesite concentrations in the precipitated solid (in wt %) as function of reaction temperature (in °C). The data displayed are average values for each reaction temperature. Error is not shown for mineral concentrations at 220 °C because no repeat analysis was performed. The error on the magnesite content at 150 °C is within the symbol size.

Figure 2. Lithium isotope fractionation factor between the precipitated solid and the solution ($10^3 \cdot \ln \alpha_{\text{prec-sol}}$) as a function of a) dolomite and b) magnesite contents (in wt %).

Figure 3. The distribution coefficient of Li between solid and solution ($D_{[\text{Li}]_{\text{prec-sol}}}$) as a function of a) dolomite and b) magnesite contents (in wt %).

Figure 4. Lithium isotope fractionation factor as a function of the reaction temperature, T (in K). Average values for each temperature are shown. The dotted line shows the linear regression through these values according to Eq. (2). Error is not shown for the isotope fractionation factor at 220 °C because no repeat analysis was performed.

Figure 5. a) Lithium isotope compositions and b) Al/Mg ratios of solutions from dolostone leaching, as a function of their HCl concentration. Decreasing $\delta^7\text{Li}$ values with increasing HCl concentration suggest a release of isotopically light Li from clay minerals, which is supported by the increase in Al/Mg ratios. Error bars are within the symbol size, if not shown.

Figure 6. Lithium isotopic compositions of solutions from dolostone leaching, as a function of their (a) Li/Ca and b) Li/Mg ratios. Error bars are within the symbol size, if not shown.

Figure 7. Lithium isotope composition of leaching solutions for experiments with HCl and acetic acid.

Figure 8. Lithium isotope composition of leaching solutions as a function of their HCl concentrations. Triangles and circles show the composition of solutions used to leach a Neoproterozoic dolostone and a modern coral, respectively. The square shows the composition of the coral total dissolution. Both coral and dolostone solutions show similar trends, suggesting release of silicate-bound Li at higher HCl concentrations. This is surprising since the coral is almost exclusively aragonite, so the release of isotopically light Li is not expected. This also implies that total dissolution in dilute HNO_3 does not release isotopically light Li into solution, although no residue was observed during dissolution in dilute HNO_3 .

Figure A1. Lithium isotope composition of solutions from coral leaching, as a function of their Li/Ca ratio. Unlike for the dolostone, there is no relationship between $\delta^7\text{Li}$ and Li/Ca. This could indicate that the isotopically-light Li is bound to a fraction with a Li/Ca similar to that of aragonite. Error bars are within the symbol size, if not shown.



Tables

Table 1. Reaction temperatures and mineral content from the precipitation experiments

Sample ID	Reaction time (days)	T (°C)	magnesite	dolomite	dolomite: magnesite
LiDol – 150 – 4.1	150	150	18.0	82.0	4.56
LiDol – 150 – 4.2	150	150	34.0	66.0	1.94
LiDol – 150 – 4.3	150	150	30.0	61.0	2.03
LiDol – 180 – 4.1	150	180	31.0	69.0	2.23
LiDol – 180 – 4.2	150	180	64.0	36.0	0.56
LiDol – 220 – 3	100	220	83.0	17.0	0.20

Mineral content in wt %. Note a maximum reaction time of 100 days was only possible at 220 °C, since no reacting solution was left after this time.

Table 2. Li isotope compositions solutions and precipitated solids for the precipitation experiments

Sample ID	Temperature (°C)	$\delta^7\text{Li}$ solution (‰)	$\delta^7\text{Li}$ solid (‰)	$10^3\ln(\alpha_{\text{prec-sol}})$	$D_{[\text{Li}] \text{ prec-sol}}$
LiCl reactive solution	-	7.85	-	-	-
LiDol - 150 - 4.1	150	7.87	0.03	-7.81	7.01
LiDol - 150 - 4.2	150	8.34	-0.63	-8.93	6.00
LiDol - 150 - 4.3	150	8.79	-0.10	-8.86	7.19
LiDol - 180 - 4.1	180	9.48	2.88	-6.56	4.66
LiDol - 180 - 4.2	180	7.88	1.71	-6.14	4.85
LiDol - 220 - 3	220	7.87	3.08	-4.77	4.92

External uncertainty (at the 2σ level) is 0.86 and 1.2 ‰ on the $\delta^7\text{Li}$ values of precipitated solids and solutions, respectively.



Table 3. Lithium isotope compositions of solutions from the dolostone and coral leaching experiments with HCl and HAc

HCl concentration (M)	$\delta^7\text{Li}_d$ (‰)	$\delta^7\text{Li}_c$ (‰)
0.05	9.46	20.1
0.10	8.00	20.2
0.15	7.27	20.2
0.20	7.13	19.5
0.30	7.62	19.3
0.50	7.04	17.8
0.80	6.78	7.04
1.00	6.29	16.7
6.00	4.00	16.9
total dissolution	n/a	20.6
HAc concentration (%)	$\delta^7\text{Li}_d$ (‰)	
0.5	10.9	
2	8.37	

$\delta^7\text{Li}_d$ and $\delta^7\text{Li}_c$ are the Li isotope composition of solutions from dolostone and coral leaching experiments, respectively.



Figures

Figure 1

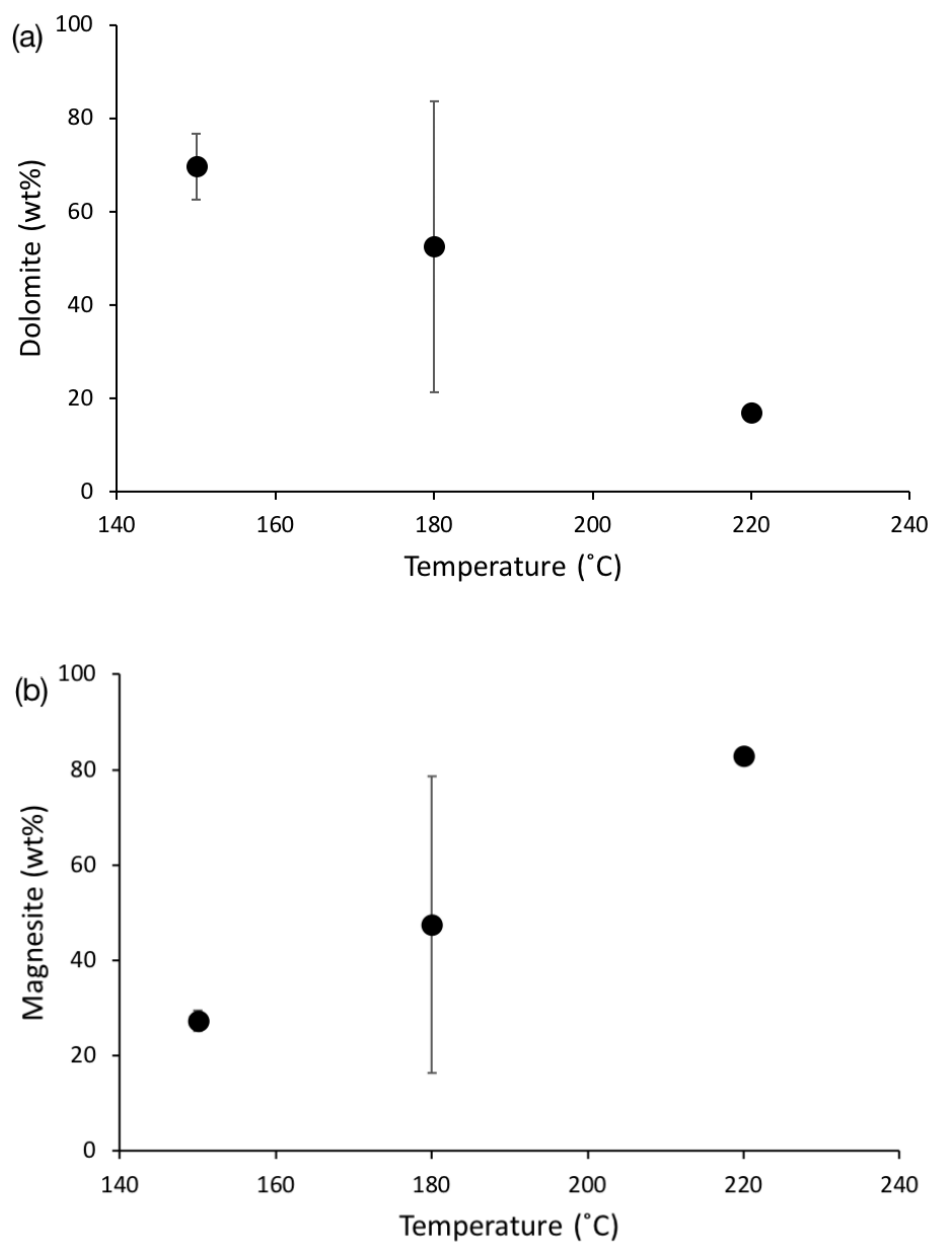




Figure 2

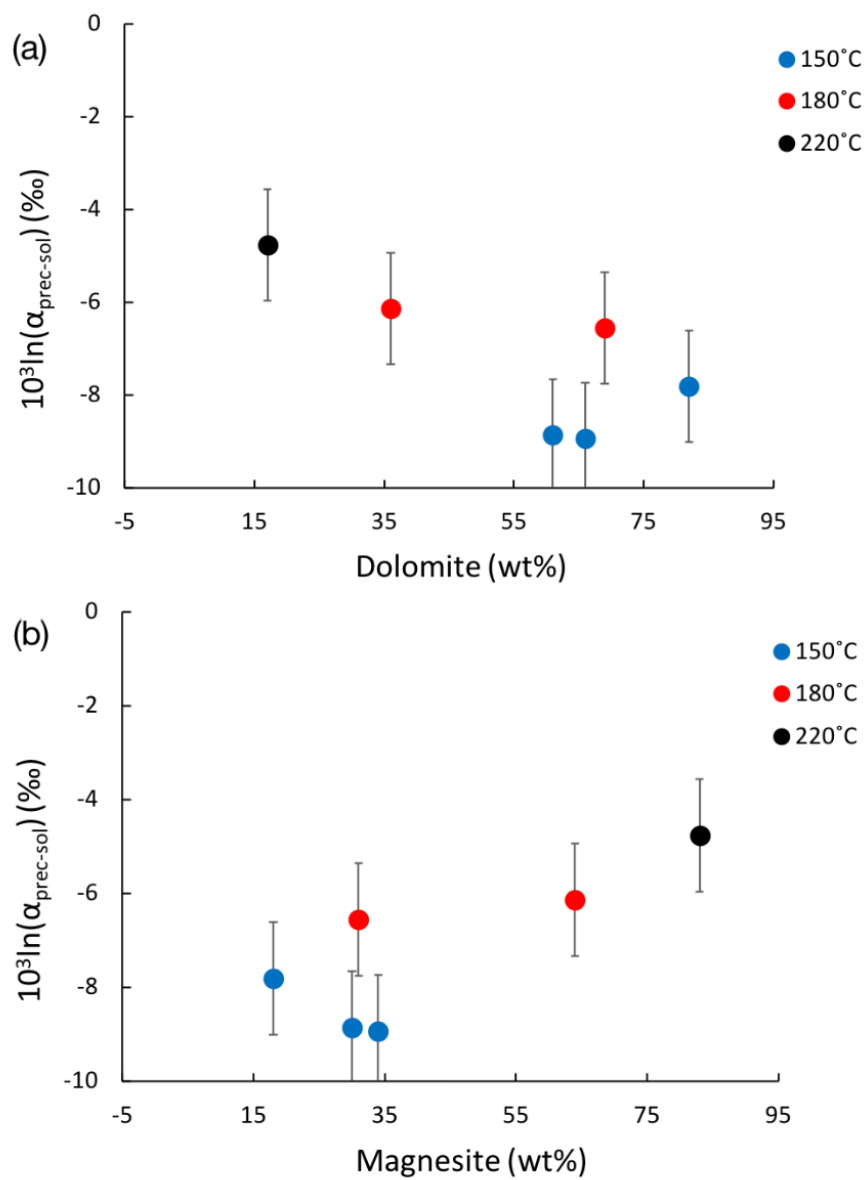




Figure 3

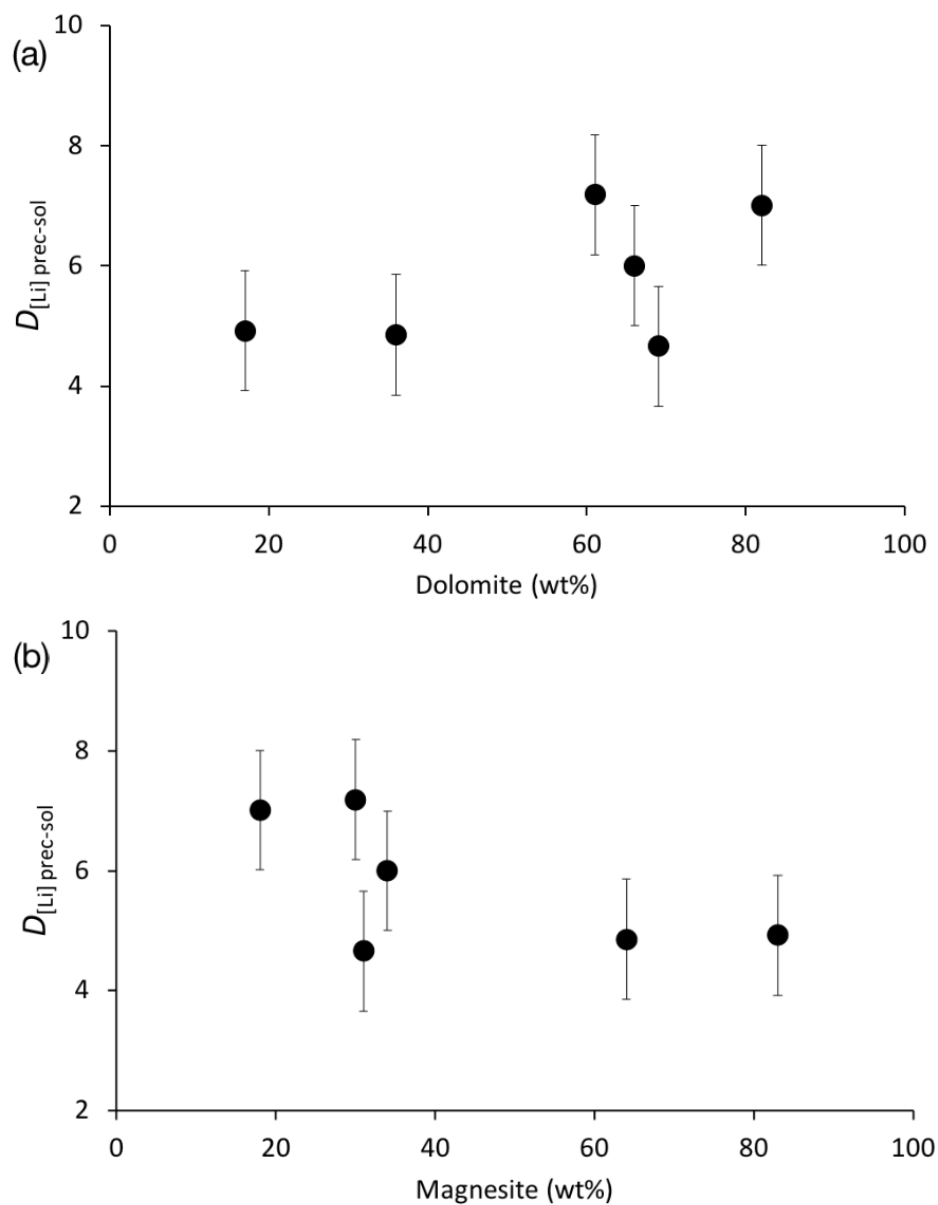




Figure 4

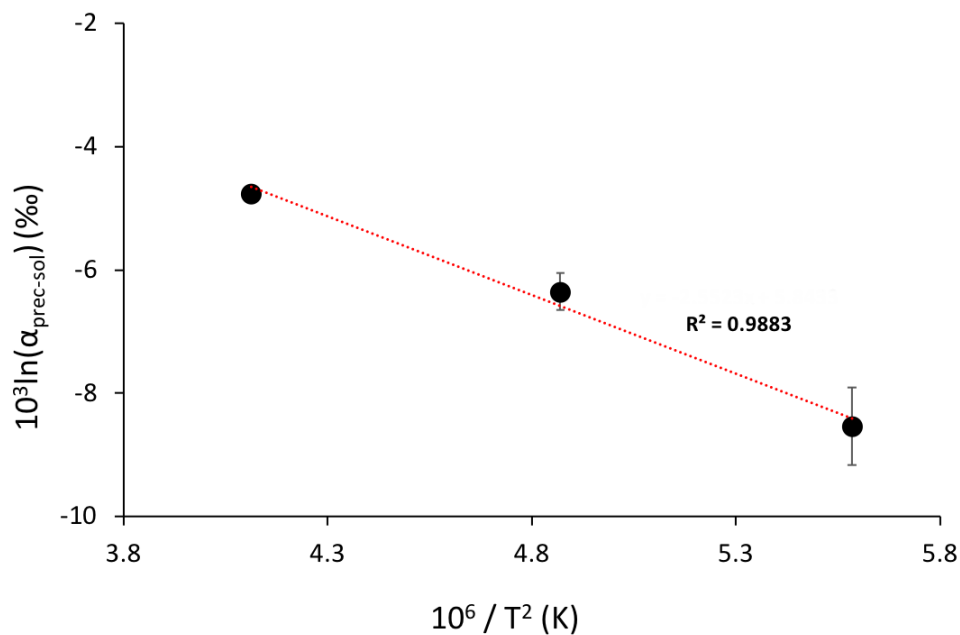




Figure 5

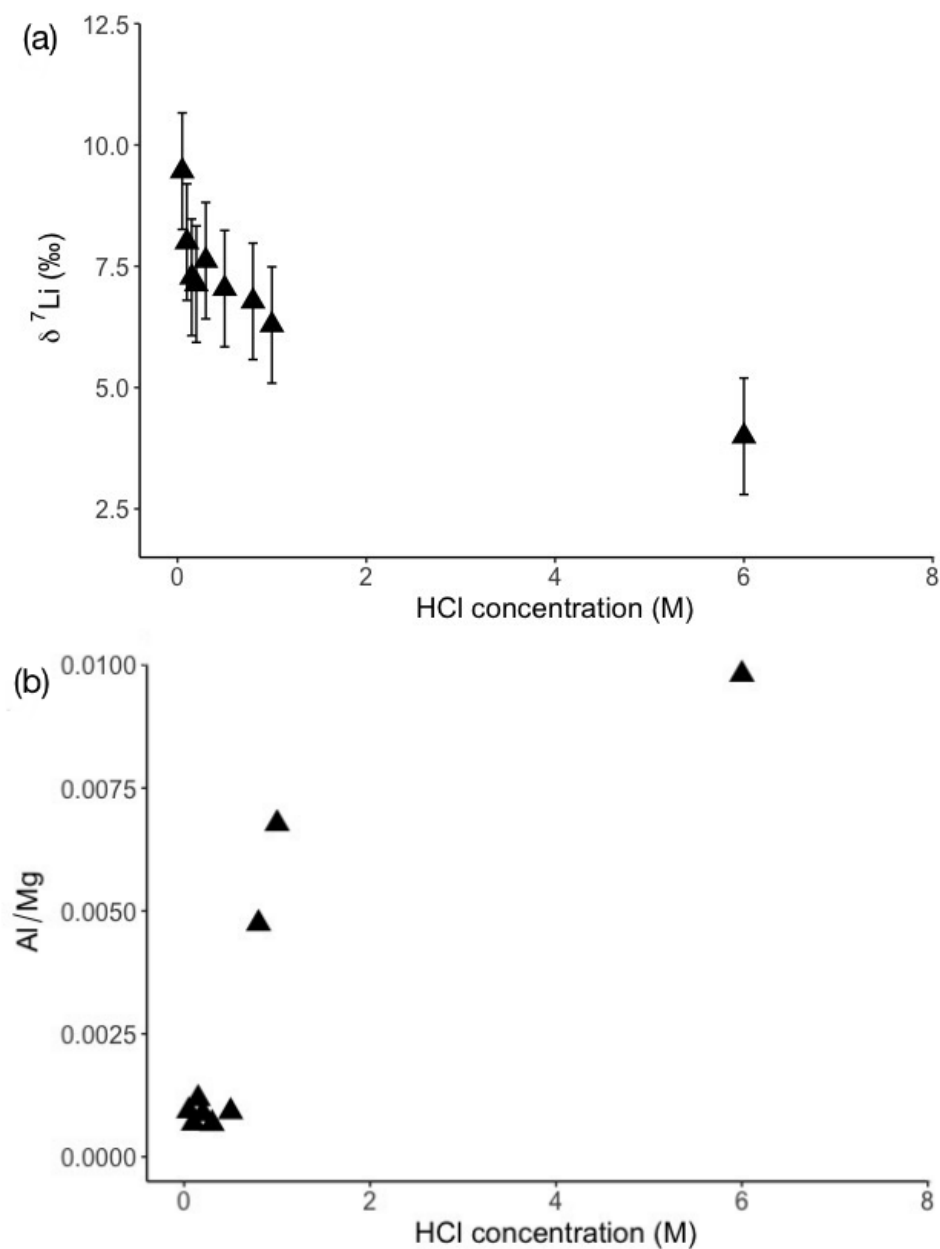




Figure 6

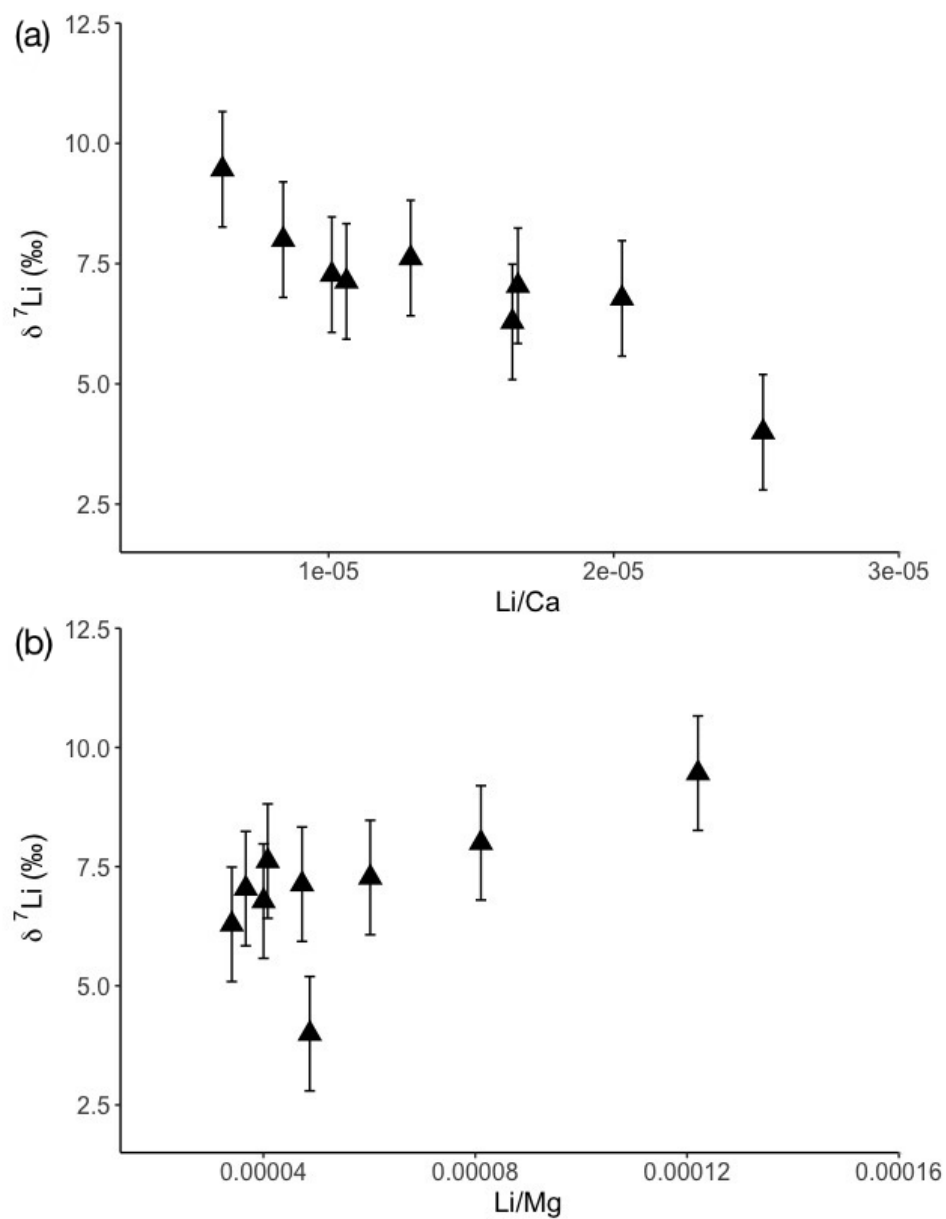




Figure 7

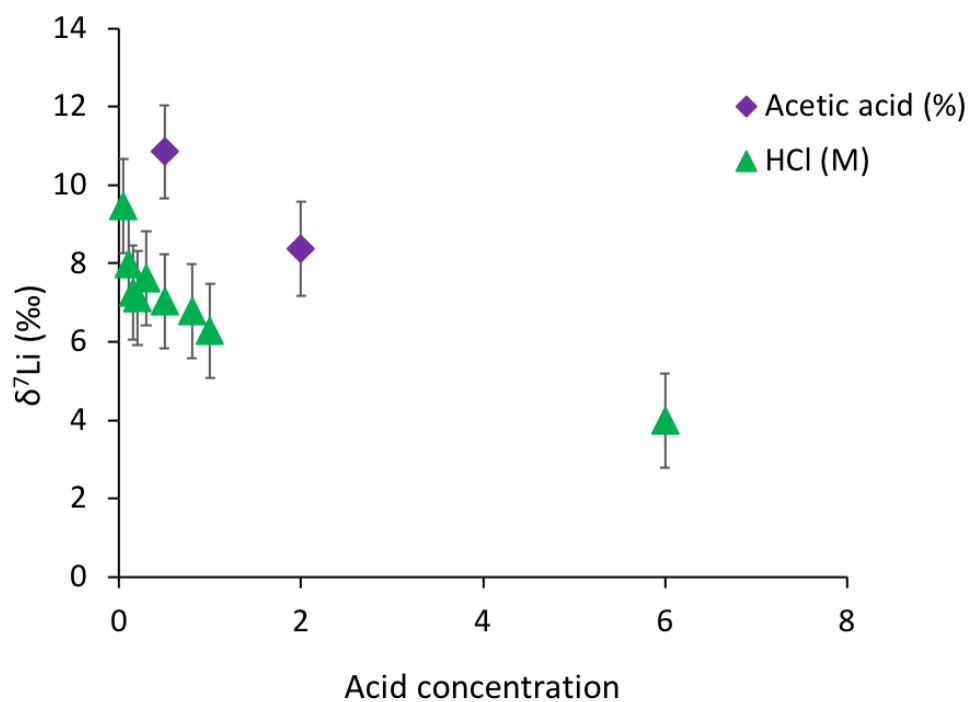




Figure 8

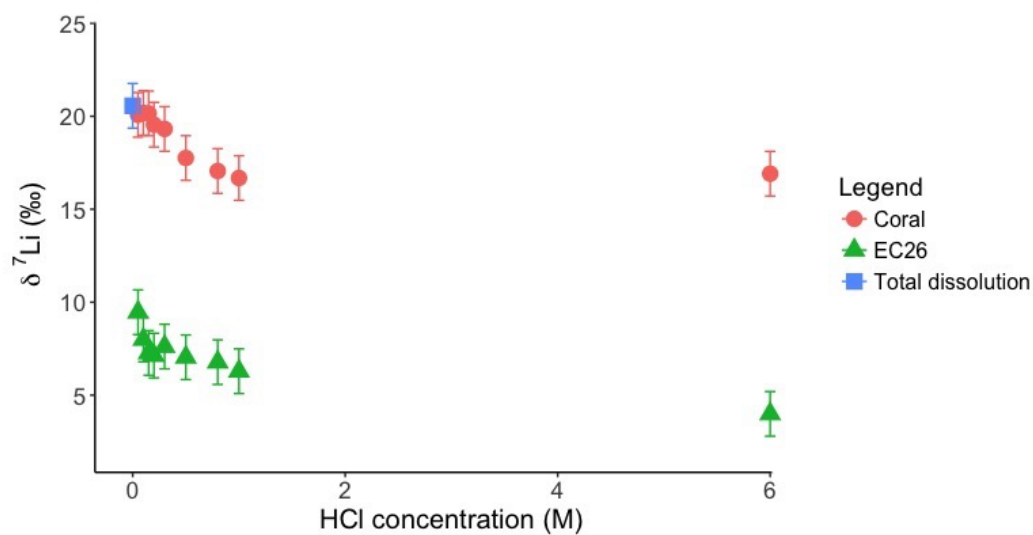




Figure A1

